Proposed Multiple Reconfigurable Intelligent Surfaces to Mitigate the Inter-User-Interference Problem in NLOS

Bushra Jarjees Qeryaqos, and Saad Ahmed Ayoob

Abstract—**Reconfigurable Intelligent Surfaces (RIS) are gaining significant global interest as a potential technology that could enable 6G. An efficient method employs passive element reflectors to extend coverage of the non-line of sight (NLOS) millimeter-wave (mm-wave) signal. The suggested model depicts a communication situation involving many users utilizing the RIS in the presence of impediments obstructing the direct path between the users and the transmitter. There is no unobstructed visual connection between sending the message and the person receiving it. The RIS enables communication using an oblique line of vision. Inter-user interference (IUI) refers to the interference that occurs when numerous users are active in the same region, which affects the received signal of a single user. Multiple remote inspection systems (RISs) of different heights have been suggested as potential solutions for addressing this issue. The results illustrate the impact of interference among users in a communication system supported by a reconfigurable intelligent surface (RIS) at various elevations in a millimeter-wave environment. Furthermore, the findings demonstrate that this idea effectively reduced the impact of the IUI. The Signal-to-Interference-plus-Noise Ratio (SINR) was enhanced for all users. The improvement percentages for the first, second, and third users are 46%, 40%, and 38%, respectively.**

Index Terms—**Reconfigurable intelligent surfaces, mm-wave environment, signal-to-interference-plus-noise ratio, RIS height, VLOS.**

I. INTRODUCTION

THE author has shifted its attention to unallocated high-frequency bands like the terahertz bands (0.1–10 THz) and millimeters wave (mm-wave) (30–100 GHz) lately due to the sharp rise in the need for high data rates [1]. The terahertz and mm-wave frequency bands provide exceptional peak data rates and an abundance of the spectrum [2]. The benefit does not come without cost because of air attenuation and transmission distance; signals at higher frequencies are more vulnerable to path loss deterioration [3]. Mm-wave bands are more vulnerable to stationary and moving obstructions than their sub-6 GHz counterparts because of their high penetration loss [4], which can even approach 40 dB for some materials, like tinted glass. Using passive reflectors to establish alternate signal routes could be one way to address the obstruction issue [5]. The SINR improvement uses several methods, like the coordinated multipoint (CoMP) technique, beamforming by designing highly efficient antennas, and using RIS. One of the viable candidate technologies for Beyond 5 Generation (B5G) communication networks is the reconfigurable intelligent surface (RIS), which is simple to implement on existing infrastructure [6-9]. A new category of planar metamaterial structures known as RISs can process and reflect electromagnetic waves that fall upon them [10]. The proposed RISs aim to improve communication performance through the intelligent regulation of wireless channels [11]. Because of its flexibility in modifying the wireless channel, RIS has been attracting much attention globally as a potential 6G-enabling technology [12]. It will be possible to overcome unwanted propagation phenomena in cellular environments economically by distributing these intelligent surfaces throughout the network [13]. Intelligent reflecting surfaces (IRS) are a unique and cost-effective way to achieve high spectrum and power savings for wireless communications using only inexpensive reflecting elements [14]. By utilizing RIS's advantages, such as providing a spectrum [15], low cost, energy consumption [5], and negligible noise [11], it is possible to overcome blockage and achieve a high range gain [16], lessening the impact of several undesirable wireless channel phenomena, like the Doppler effect and multipath fading by RIS [17], and might function as a receiving or sending node [18]. Using passive element reflectors is a new method to cover the NLOS mm-wave signal. Electromagnetic waves have great reflecting qualities at higher frequencies due to their smaller skin depth and lower material penetration. Also, there is less diffraction near reflector edges at mm-wave frequencies [19]. Multipath fading causes excessive signal fluctuations, and the big obstacle presence leads to a complete interruption of the wireless link between the desired user and the transmitter due to the dynamic nature of the wireless environment [20]. RISs reverse accident signals to

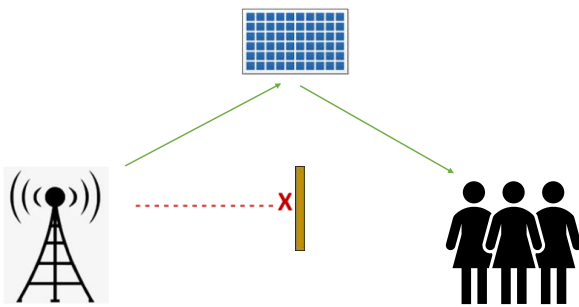solve this issue and increase users' SINR, as illustrated in Fig.1.

Fig. 1. Virtual line-of-sight path (VLOS) via RIS

Using RIS/IRS, it is possible to increase the coverage area, raise channel rank, reduce interference, and increase reliability and positioning accuracy [21]. The term "reflection" in this sense refers to a wide range of phenomena [22], such as perfect reflections that are specular (from an ideal mirror, for example) and scattered refraction (from a rough surface, for example). When electromagnetic waves hit a rough surface, they often spread in all directions [23]. Smooth surfaces reflect the wave in the direction of the specular plane. There's no distraction. This paper discusses the RIS device, which collects the electromagnetic (EM) wave impinging on it and reflects the collision signal in the receiver direction [24]. RIS does not amplify the transmitted signal, but it is capable of creating intelligent radio environments through it. It can also control the propagation environment it provides [25]. To comply with green communications requirements, RISs are environmentally friendly [26].

The main contributions of this paper include the following:

1. Optimizing reconfigurable intelligent surfaces (RIS) sites to improve the signal-to-interference plus noise ratio in state non-line of sight (NLOS) communication.
2. Proposing a communication model in 3D consisting of multiple RISs placed vertically to reduce inter-user interference (IUI) and increase the signal-to-interference plus noise ratio.

The paper featured several main paragraphs following the introduction, which included relevant research related to the content of this manuscript. The third paragraph contained the communication model between the transmitter and receiver using a virtual line of sight (VLOS). The results and discussion are in the fourth paragraph. Finally, the conclusions are in the fifth paragraph.

II. RELATED WORK

A system formed from multiple RISs and massive multi-input/multi-output (mMIMO) for many users was studied, with the study's goal being to maximize SINR. The authors studied two methods for zeroing interference at users (UEs) and RISs using zero-force beamforming (ZF), namely BS-UE-ZF and BS-RIS-ZF. Hardware impairments (HWIs) have minimal impact on the SINR, and STAR-RIS yields superior results over traditional RIS [27]. Moreover, it highlights the effect of HWIs

with a focus on single-cell downlinks and analyses the minimum SINR produced by the optimal linear precoder (OLP) with HWIs [28]. In [29], the authors employ phase shift enhancement techniques for RIS-assisted MIMO radar. The authors combine transmission beam patterns to maximize SINR in MIMO radar and introduce an optimization technique. The phase transformation optimization process used a specialization minimization (MM) technique using first-order Taylor expansion. In addition, compare RIS-assisted MIMO radar to standard MIMO radar. The results show that the SINR significantly increased. In [30], The purpose was to maximize the minimal SINR of uplink RIS-aided communication by proposing a shared optimization technique for beamforming, RIS phases, and power allocation.

Furthermore, suggest two methods for optimizing the phase shifts at the RIS: one that depends on the minimal function approximation, and the other is based on the matrix lifting method. Additionally, it suggests a heuristic approach to maximize the values of the quantized phase shift. The proposed approach, compared to a system with random RIS stages, achieves a minimum SINR gain of more than 300%, according to the results. The power reduction problem under the SINR requirements for all users' needs hybrid beamforming at the BS and the response matrix at the RIS to be optimized simultaneously. A sequential optimization method with minimal complexity proposes to optimize the digital beamformer, the analog beamformer, and the RIS reflection coefficients. The results [31] show that RIS influences significant power loss. This study, in [32], focuses on the downlink of a single-cell multi-user system in which users connect with a base station (BS) via a RIS that has a line of sight (LOS) with the BS. It analyzed the lowest SINR that an optimal linear precoder (OLP) could obtain. The simulations show that RIS devices need to be big to work better than full-duplex relays, but they can work better than half-duplex relays with only a few passive reflective elements.

In this paper, we test how signal interference from other users affects a single user's SINR level, show how the height and location of the RIS affect the SINR level, and suggest multiple RIS systems to reduce inter-user interference in NLOS environments.

III. THEORETICAL AND SYSTEM MODEL

A significant amount of traffic in future access networks uses the millimeter wave (mm-wave) spectrum, which has more bandwidth than other available bandwidths [33]. The mm waves have short wavelengths, and high frequencies and do not travel over a large area. High-frequency radio can be easily blocked, increased susceptibility to path loss, and poor propagation conditions [34]. Experts have suggested Reconfigurable Intelligent Surfaces (RISs) as a potential solution to the obstruction problem. RISs are especially helpful when the LOS link is blocked or poorly reliable. RISs enable the provision of transmission pathways by utilizing their reflecting parts [35].

The proposed model describes the communication situation for multiple users through the RIS, where obstacles exist

between the transmitter and the users. In other words, there is no LOS path between the transmitter and the receiver. The RIS provides a non-line-of-sight (NLOS) path for active communication. The RIS introduces a new path known as the virtual line-of-sight path (VLOS). RIS consists of a set of passive reflective elements. It is a passive reflective surface in the form of a rectangle, meaning it does not require power. It reflects the electromagnetic signal coming from the transmitter to the user. Table I shows the recurring parameters and symbols.

Fig. 2 shows the details of the studied system model in terms of significant dimensions and abbreviations. It is assumed that there are six users on the receiving side.

TABLE I
THE RECURRING PARAMETERS AND SYMBOLS.

Symbol	Explanation	SYMBOL	Explanation
f	Operating frequency	η	The efficiency of RIS
λ	wavelength	dx/dy	Dimensions along the x and y axis of the RIS elements, respectively
Pt	Power Transmitted	Rts	The diagonal dimension between Tx and RIS
w	Signal bandwidth	Rsr	The diagonal dimension between RIS and RX
F_{dB}	Noise Figure	dl	The horizontal distance between Tx and RIS
N_0	power of thermal noise	$d2$	The horizontal distance between RIS and RX
hs	The height of the RIS relative to the earth	$\theta i/\theta r$	Incidence and reflection angles, respectively, relative to the RIS
ht/hr	TX, RX height relative to the earth	A	The area of RIS
Gt/Gr	TX, RX antenna gain	Pr	Power Received
Pi	Power Interference	x	The dimension of the RIS from the TX-RX line
σ	The cross-section of the RIS	η	The efficiency of RIS
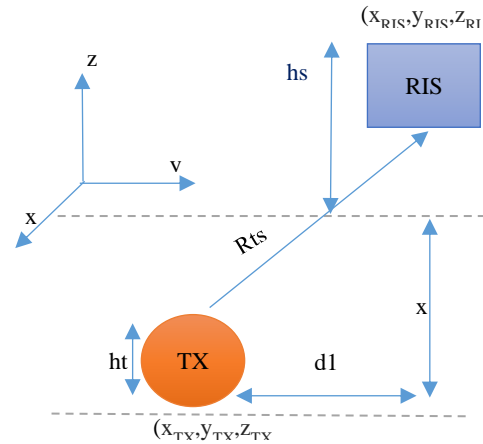
(a) The dimensions on the Transmitter's side.
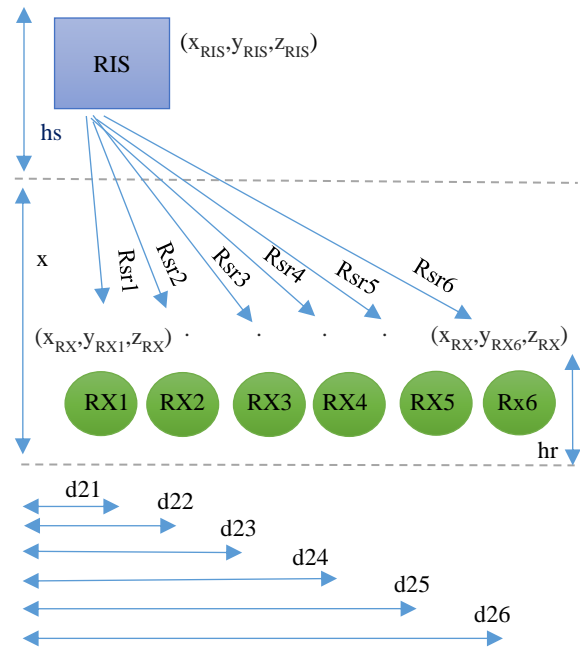
(b) The dimensions on the Receiver's side.

Fig. 2. Inter-User Interference (IUI) situation.

The coordinates of the transmitter, receivers, and RIS are (x_{TX}, y_{TX}, z_{TX}), (x_{RX}, y_{RX1}, z_{RX}), (x_{RX}, y_{RX2}, z_{RX}), (x_{RX}, y_{RX3}, z_{RX}), (x_{RX}, y_{RX4}, z_{RX}), (x_{RX}, y_{RX5}, z_{RX}), (x_{RX}, y_{RX6}, z_{RX}), and (x_{RIS}, y_{RIS}, z_{RIS})), respectively. The horizontal distance between Tx and RIS is dtsh or d1. The symbol dsrh or d2 represents the horizontal distance between RIS and RX, the symbol Rts represents the TX-RIS diagonal dimension. Finally, the symbol Rsr represents the diagonal dimension between RIS-RX. The model relies heavily on the TX, RIS, and RX heights, denoted as ht, hs, and hr. This model proposed three RIS heights, symbolized by hs1, hs2, and hs3, to improve the signal-to-interference plus noise ratio. The transmitted signal in VLOS is subjected to incidence and reflection angles θi and θr, respectively as seen in the Fig. 3.

As mentioned earlier, there is an obstacle between the transmitter and the receivers, and there is an NLOS path. The transmitter will send the signal to the RIS. The RIS will do its job of relaying this signal to the receivers. These require that the position of the RIS be between the transmitter and the receivers, provided that the Tx and Rx (1-6) are on the same side to allow the RIS to reflect the signal from the transmitter towards the receiver [36]. On one side, the transmitter and RIS must be in LOS, and on the other, the RIS and receiver must also be in LOS. To ensure this, the RIS must be higher than the transmitter and receiver heights [37].
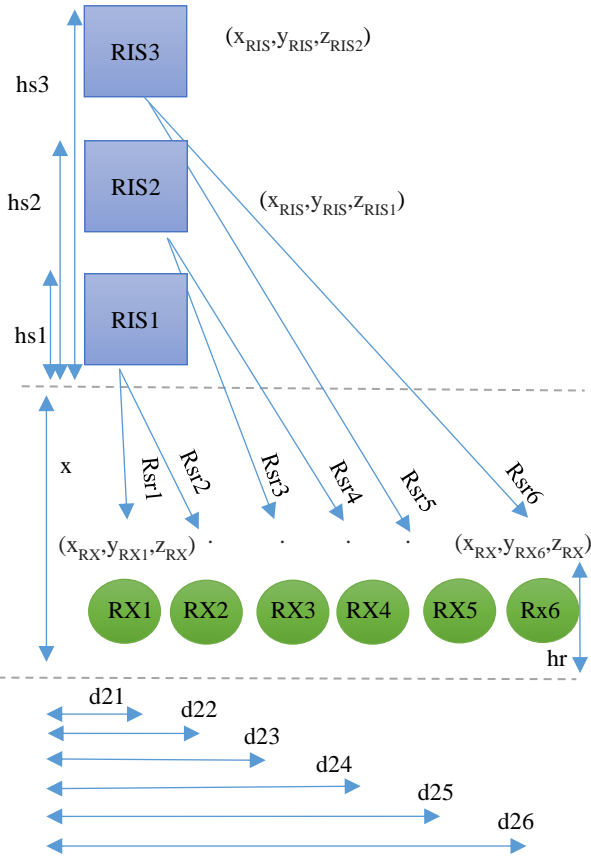
Fig. 3. Proposed system model (receiver's side).

The RIS aids in determining the SINR at the receiver. Next, data analysis will determine the optimal RIS position that yields the highest SINR value. It is worth noting that the height of the transmitter is higher than the receiver's. In addition, path losses are significant. The surface is highly efficient and reflects the signal without any loss. We will calculate the received power by placing the RIS between TX and RX, as shown in equation below [38]:

$$Pr = \frac{Pt \; Gt \; Gr \; \lambda^2 \; \sigma}{(4\pi)^3 Rts^2 Rsr^2} \tag{1}$$

Pt is the transmitted power by the TX. Gt and Gr are the gains of the TX and RX antennas, respectively. The transmitted electromagnetic wave's wavelength is λ. TX-RIS and RIS-RX have two dimensions: dts and dsr. σ is the cross-section of the RIS that approximates a rectangular, planar surface. Detailed as follows:

$$\sigma = \frac{4\pi\eta Cos\theta i Cos\theta r A^2}{\lambda^2} \tag{2}$$

The efficiency of the RIS η refers to the ratio of the power of the signals it transmits to the signals it receives [39]. A is the area of RIS. θi and θr represent the incident and reflected angles for the signal transmitted, respectively. It is assumed in this paper that RIS consists of passive elements with η = 1[35]. By substituting (2) into (1), the first equation takes on the following form:

$$Pr = \frac{Pt \; Gt \; Gr \; \eta \; A^2 Cos\theta i \; Cos\theta r}{(4\pi)^2 Rts^2 Rsr^2} \tag{3}$$

In light of the analysed calculations, it is easy to determine the following:

$$dts = \sqrt{d1^2 + x^2 + (hs - ht)^2} \;\; and$$

$$dsr = \sqrt{d2^2 + x^2 + (hs - hr)^2} \tag{4}$$

$$\theta i = tan^{-1}\left(\frac{\sqrt{d1^2 + (hs - ht)^2}}{x}\right) \;\; and$$

$$\theta r = tan^{-1}\left(\frac{\sqrt{d2^2 + (hs - hr)^2}}{x}\right) \tag{5}$$

Inter-user interference (IUI) occurs when several users in the same area interfere with the received signal for a single user. In this scenario, beamforming technology directs the signal directly towards a specific receiver. Using this technology reduces user interference [40, 41]. Simultaneously, it can direct the beam in the desired direction or at the desired angle's target point [5]. Unfortunately, there is still an inter-user interference effect because users are closer together. We propose to solve this issue by deploying the RIS at three different heights. The transmitting antenna is of the planer array antenna type consisting of M×N elements, placed in the direction of the x and y axes, where dx and dy are the spacing between antenna elements equal to λ/2. Im, and In are current amplitudes. k = 2π/λ, where λ is the wavelength. The array radiation factor in any direction can be defined as follows if the excitation current in each row has the same distribution pattern [42]:

$$AF_n = AF_X \cdot AF_y = \left(\frac{1}{M} \frac{I_m \sin\left(\frac{M}{2}\psi_x\right)}{\sin\left(\frac{\psi_x}{2}\right)}\right)\left(\frac{1}{N} \frac{I_n \sin\left(\frac{N}{2}\psi_y\right)}{\sin\left(\frac{\psi_y}{2}\right)}\right) \tag{6}$$

where: $\psi_x = K \, d_x \, \sin\theta \cos\phi + \beta_x$,

$\psi_y = K \, d_y \, \sin\theta \cos\phi + \beta_y$ and

$\beta_x = -K \, d_x \, \sin\theta_o \cos\phi_o$, $\beta_y = -K \, d_y \, \sin\theta_o \sin\phi_o$.

The following formula determines inter-user interference power:

$$Pi = \frac{Pt \; Gt \; Gr \; \eta \; A^2 Cos\theta \; Cos\theta r}{(4\pi)^2 Rts^2 Rsr^2} \tag{7}$$

According to the equation above, Gt and Gr represent transmitted and received gains, and we compute Gt using Gt = AF² Gtmax [43, 44]. As a result, the receiver's similar end-to-end SINR can be calculated as follows:

$$SINR = \frac{Pr}{N_0 + Pi} \tag{8}$$

Lastly, consider the presence of additive white Gaussian noise in the received signal, symbolized by N_0 that the following equation uses to calculate it [37]:

$$N_o = -174 + 10 \, log_{10}(w) + F_{dB} \qquad (9)$$

where W is the transmission bandwidth, and F_{dB} is the noise figure in dB.

IV. RESULTS AND DISCUSSION

This section contains results demonstrating the effect of interference between users in a communication system supported by RIS in a mm-Wave environment in two cases: the first the users are in the middle of the cell and the second the users are in the edge of the cell. These results are obtained using Eq. (7) to validate the proposed system through the simulation program MATLAB, as illustrated in Fig. 2. Table II presents the specific simulation parameters utilized in the proposed model.

TABLE II
THE PARAMETERS OF THE PROPOSED MODEL.

Parameter	Value	Parameter	Value
f	28 GHz	η	100%
Pt	1 W	Gt	40 dB
W	2 GHz	Gr	10 dB
F_{dB}	10 dB	ht	12 m

A. Users in the Middle of the Cell

Increasing the number of RISs at various heights reduces interference between users. Fig. 4. illustrates the effect of RIS height on the SINR of the signal transmitted to users at varying distances from the TX. For example, the first user is very close to the TX, among second range users, the second user is the furthest from the first, and so on until the last sixth user is the furthest from the TX. This explains the need for different heights for RIS, i.e., low height for nearby users, higher height for farther users, and high height for distant users. The peak SINR values that occur at a certain RIS height for each user mean that at this height, the RIS is appropriate for the distance of this user and gives the maximum value of SINR. Note that the SINR decreases with increasing distance. Where $\emptyset = tan^{-1}\frac{d2}{x}$, that is, the angle between the user's distance from the middle of the distance between TX and RX and the RIS's distance from the TX-RX line.

This paper uses RIS at three specific heights: hs1 = 33 meters, hs2 = 48 meters, and hs3 = 78 meters. These three heights are proportional to the user's distance from the TX and at a specific distance x of 50 meters, which represents the distance between the Tx-RX line and the RIS. At these values, Fig. 5. (a) shows the effect of the first RIS height on SINR, with a gradual increase in the number of users. From Fig. 5 (a), it appears that this height is suitable for users close to the TX. Fig. 5 (b) shows that the second height is suitable for users who are at a moderate distance from the TX and Fig. 5 (c) shows that the third height is suitable for users far from the TX but does not serve users that are very far away (i.e., farther than 20 m).
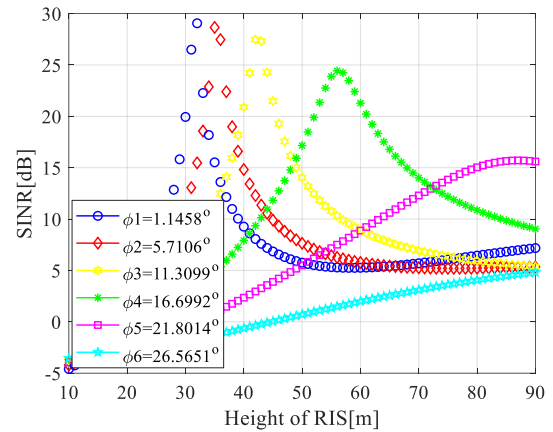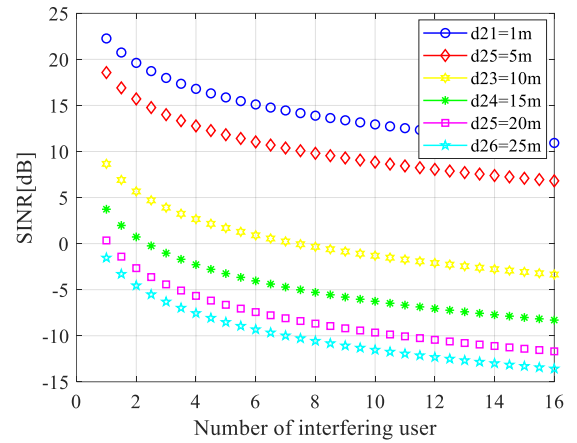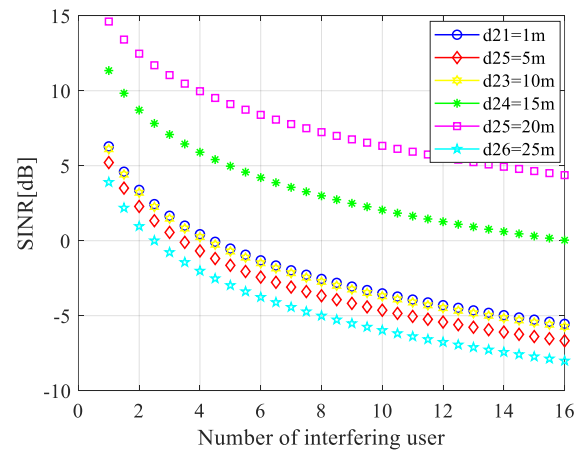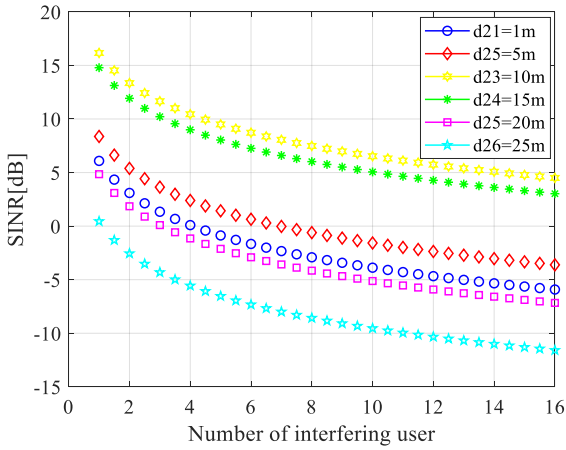

Fig. 4. SINR varies RIS height at x=50m.

(a) x = 50m, hs = 33 m.

(b) x = 50m, hs = 48 m.

(c) x = 50m, hs = 78 m.

Fig. 5. SINR varies with the number of interfering users at x = 50 m.

Table III shows the SINR values before and after adding the first height of the RIS. It is easy to find that the SINR improvement for the first and second users is 46% and 40%, respectively. The SINR is neglected for the user's rest because the height of 33m serves the nearby users. The SINR values for users of medium dimension improve when adding RIS with a height of 48 m; for the third and fourth users, they are 38% and 22%, respectively.

TABLE III
THE SINR VALUES BEFORE AND AFTER ADDING THE FIRST
HEIGHT OF THE RIS.

SINR	AT HS=30M, BEFORE	AT HS=33M, AFTER
SINR1	19.9393 dB	22.2677 dB
SINR2	11.0812 dB	18.5663 dB
SINR3	5.7508 dB	8.6584 dB
SINR4	2.2553 dB	3.7301 dB
SINR5	-0.4425 dB	0.3451 dB
SINR6	-1.9103 dB	4.1448 dB

B. Users at the Edge of the Cell

Conclusion: Changing the RIS height alone cannot achieve the best SINR for all users, regardless of their position. Therefore, we proposed a new RIS position, changing the value of X from 50 meters to 10 meters, to cater to the needs of users who are very distant. Fig. 6 shows that the new location of the RIS place at x = 10 meters is suitable for very (for example > 85m) and very close (for example <15m) users but not for other users.

We have now chosen a height of 9 meters for the RIS. It turns out that this location and height are suitable for both very close and very far users. However, if serving only very remote users is the goal, we can increase the RIS height to 12 meters to achieve the maximum SINR value, as illustrated in Fig. 7.

Finally, it can be said that the distance x has a very significant effect on the transmitted signal as well as the height of the RIS. If the distance x is large (for example =50 m) and the RIS is at
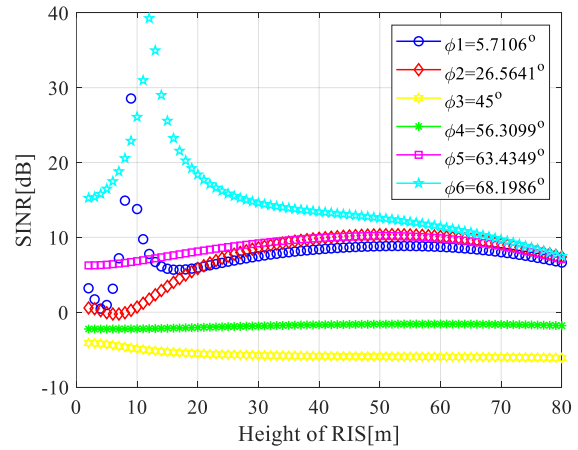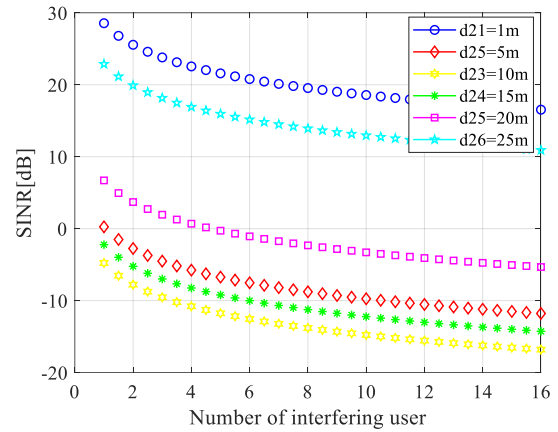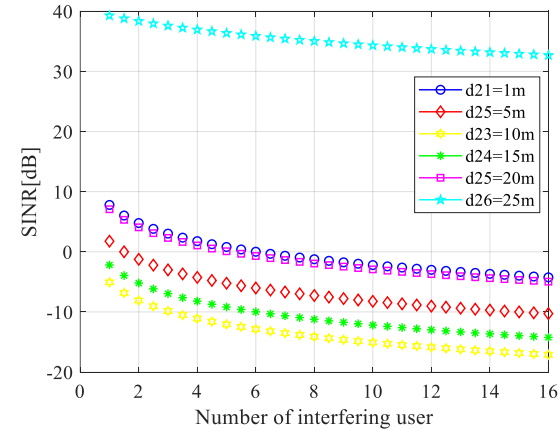

Fig. 6. SINR varies RIS height with different user positions at x=10m.

(a) x = 10m, hs = 9 m.

(b) x = 10m, hs = 12 m.

Fig. 7. SINR varies with the number of interfering users at x = 10 m.

three different heights, each height serves users with different dimensions than TX. This RIS side serves users in the middle of the cell. If the distance x is low (for example = 10 m) and the height of RIS is low, the very close and very distant users will benefit, but if the distance is low and the RIS is slightly higher than before, it only serves the very distant users. That is, the

nearby RIS site serves users at the cell's edges. Table IV shows the comparison of this paper with other papers. The comparison includes several metrics, including: frequency band, Number of RIS, type of communication path and etc.

TABLE IV
THE COMPARISON OF THIS PAPER WITH OTHER PAPERS.

Main contents		[5]	[12]	[31]	[37]	THIS WORK
Frequency band		28 GHz	35 GHz	28 GHz	140 GHz	28 GHz
Deployment	Single-user	✓	✓			✓
	Multi-user			✓	✓	✓
Number of RIS	Single	✓	✓	✓	✓	
	Multi					✓
Com. path	LOS					
	NLOS	✓	✓	✓	✓	✓
Environment	Out door	✓	✓	✓	✓	✓
Measures	SNR	✓	✓			✓
	SINR			✓		✓

Regarding Figures 5 and 7, the SINR generally increases as x decreases, however, according to equations 5 (the effect is +ve on incident & reflected angles and as a result -ve on Pr & Pi) and 4 (the effect is -ve on Rts & Rsr and as a result +ve on Pr & Pi). So, this can be justified by saying that the effect of distances is higher than the effect of angles on Pr & Pi.

V. CONCLUSION

This paper was concerned with reducing the interference resulting from the intersection of several beams when using a single RIS in the 3D domain. Several RISs proposed to solve this problem and improve the SINR for each user. The proposed model illustrates how different user dimensions affect the SINR value. The RIS site also significantly affects the signal value, i.e., the RIS height and distance from the TX-RX line. If the RIS site is close to the TX-RX line, it serves users at the cell's edge. If the RIS site is away from the TX-RX line, it serves users in the middle of the cell. Positioning the RIS at one height at the distant site of the TX-RX line will not allow users in the middle of the cell to receive the signal at acceptable levels. The solution to this problem is to deploy three RISs on the same site at three different heights, corresponding to user dimensions. It only caters very distant users. The nearby RIS site provides users with access to the cell's edges.

REFERENCES

[1] G. Stratidakis, S. Droulias, and A. Alexiou, "Analytical Performance Assessment of Beamforming Efficiency in Reconfigurable Intelligent Surface-Aided Links," IEEE Access, vol. 9, pp. 115922–115931, 2021, doi: 10.1109/ACCESS.2021.3105477

[2] W. Tang et al., "Path Loss Modeling and Measurements for Reconfigurable Intelligent Surfaces in the Millimeter-Wave Frequency Band," IEEE Trans. Commun., vol. 70, no. 9, pp. 6259–6276, 2022, doi: 10.1109/TCOMM.2022.3193400.

[3] S. Alfattani, W. Jaafar, Y. Hmamouche, H. Yanikomeroglu, and A. Yongacoglu, "Link Budget Analysis for Reconfigurable Smart Surfaces in Aerial Platforms," IEEE Open J. Commun. Soc., vol. 2, no. June, pp. 1980–1995, 2021, doi: 10.1109/OJCOMS.2021.3105933.

[4] A. Al-Rimawi and A. Al-Dweik, "On the Performance of RIS-Assisted Communications with Direct Link Over κ-μ Shadowed Fading," IEEE Open J. Commun. Soc., vol. 3, no. December, pp. 2314–2328, 2022, doi: 10.1109/OJCOMS.2022.3224562.

[5] K. Ntontin et al., "Wireless Energy Harvesting for Autonomous Reconfigurable Intelligent Surfaces," IEEE Trans. Green Commun. Netw., vol. 7, no. 1, pp. 114–129, 2023, doi: 10.1109/TGCN.2022.3201190.

[6] S. A. Ayoob, F. S. Alsharbaty, and A. K. Alhafid, "Enhancement the heavy file application of 802.16 e cell using intra-site CoMP in uplink stream" Journal of Engineering Science and Technology, 17 (3), 1721-1733, 2022.

[7] S. A. Ayoob, F. S. Alsharbaty, and A. N. Hammodat, "Design and simulation of high efficiency rectangular microstrip patch antenna using artificial intelligence for 6G era" TELKOMNIKA (Telecommunication Computing Electronics and Control), 21(6), 1234-1245, 2023.

[8] S. A. Ayoob, F. E. Mahmood, and F. Y. Abdullah, "Design and Simulation of a High Gain Microstrip Patch Antenna for 5G Communication Systems" IEEE, Proceedings of the 2023 International Conference on Engineering, Science and Advanced Technology (ICESAT), Mosul, Iraq, 65-68, 2023.

[9] K. Singh, S. K. Singh, and C. P. Li, "On the Performance Analysis of RIS-Assisted Infinite and Finite Blocklength Communication in Presence of an Eavesdropper," IEEE Open J. Commun. Soc., vol. 4, no. April, pp. 854–872, 2023, doi: 10.1109/OJCOMS.2023.3262485.

[10] M. A. Shawky et al., "Reconfigurable Intelligent Surface-Assisted Cross-Layer Authentication for Secure and Efficient Vehicular Communications," pp. 1–12, 2023, [Online]. Available: http://arxiv.org/abs/2303.08911

[11] Z. Zhang et al., "Active RIS vs. Passive RIS: Which Will Prevail in 6G?," IEEE Trans. Commun., vol. 71, no. 3, pp. 1707–1725, 2023, doi: 10.1109/TCOMM.2022.3231893.

[12] Y. Ren et al., "On Deployment Position of RIS in Wireless Communication Systems: Analysis and Experimental Results," IEEE Wirel. Commun. Lett., vol. 12, no. 10, pp. 1756–1760, 2023, doi: 10.1109/LWC.2023.3292125.

[13] N. Simmons et al., "A Simulation Framework for Cooperative Reconfigurable Intelligent Surface Based Systems," IEEE Trans. Commun., pp. 1–31, 2023, doi: 10.1109/TCOMM.2023.3282952.

[14] Q. Wu and R. Zhang, "Beamforming Optimization for Wireless Network Aided by Intelligent Reflecting Surface with Discrete Phase Shifts," IEEE Trans. Commun., vol. 68, no. 3, pp. 1838–1851, 2020, doi: 10.1109/TCOMM.2019.2958916.

[15] E. Moeen Taghavi, R. Hashemi, N. Rajatheva, and M. Latva-Aho, "Environment-Aware Joint Active/Passive Beamforming for RIS-Aided Communications Leveraging Channel Knowledge Map," IEEE Commun. Lett., vol. 27, no. 7, pp. 1824–1828, 2023, doi: 10.1109/LCOMM.2023.3270491.

[16] Y. Wang and J. Peng, "Energy Efficiency Fairness of Active Reconfigurable Intelligent Surfaces-Aided Cell-Free Network," IEEE Access, vol. 11, no. January, pp. 5884–5893, 2023, doi: 10.1109/ACCESS.2023.3237213.

[17] Y. Bian, D. Dong, J. Jiang, and K. Song, "Performance Analysis of Reconfigurable Intelligent Surface-Assisted Wireless Communication Systems Under Co-Channel Interference," IEEE Open J. Commun. Soc., vol. 4, no. February, pp. 596–605, 2023, doi: 10.1109/OJCOMS.2023.3244648.

[18] G. Ghatak, "On the Placement of Intelligent Surfaces for RSSI-Based Ranging in Mm-Wave Networks," IEEE Commun. Lett., vol. 25, no. 6, pp. 2043–2047, 2021, doi: 10.1109/LCOMM.2021.3063918.

[19] W. Khawaja, O. Ozdemir, Y. Yapici, F. Erden, and I. Guvenc, "Coverage enhancement for NLOS mmWave links using passive reflectors," IEEE Open J. Commun. Soc., vol. 1, no. December 2019, pp. 263–281, 2020, doi: 10.1109/OJCOMS.2020.2969751.

[20] B. Yang, X. Cao, C. Huang, C. Yuen, L. Qian, and M. Di Renzo, "Intelligent Spectrum Learning for Wireless Networks with Reconfigurable Intelligent Surfaces," IEEE Trans. Veh. Technol., vol. 70, no. 4, pp. 3920–3925, 2021, doi: 10.1109/TVT.2021.3064042.

[21] C. Pan et al., "An Overview of Signal Processing Techniques for RIS/IRS-Aided Wireless Systems," IEEE J. Sel. Top. Signal Process., vol. 16, no. 5, pp. 883–917, 2022, doi: 10.1109/JSTSP.2022.3195671.

[22] O. Ozdogan, E. Bjornson, and E. G. Larsson, "Intelligent Reflecting Surfaces: Physics, Propagation, and Pathloss Modeling," IEEE Wirel. Commun. Lett., vol. 9, no. 5, pp. 581–585, 2020, doi: 10.1109/LWC.2019.2960779.

[23] J. Ma, R. Shrestha, W. Zhang, L. Moeller, and D. M. Mittleman, "Terahertz Wireless Links Using Diffuse Scattering from Rough Surfaces," IEEE Trans. Terahertz Sci. Technol., vol. 9, no. 5, pp. 463–470, 2019, doi: 10.1109/TTHZ.2019.2933166.

[24] V. Tapio, D. Jagyasi, A. Shojaeifard, P. Pirinen, and M. Juntti, "SNR-based Configuration for RIS-Integrated NR".

[25] D. Diao et al., "Reflecting Elements Analysis for Secure and Energy-efficient UAV-RIS System with Phase Errors," IEEE Wirel. Commun. Lett., no. October, 2023, doi: 10.1109/LWC.2023.3327384.

[26] X. Yuan, Y. J. A. Zhang, Y. Shi, W. Yan, and H. Liu, "Reconfigurable-Intelligent-Surface Empowered Wireless Communications: Challenges and Opportunities," IEEE Wirel. Commun., vol. 28, no. 2, pp. 136–143, 2021, doi: 10.1109/MWC.001.2000256.

[27] S. Aghashahi, Z. Zeinalpour-Yazdi, A. Tadaion, M. B. Mashhadi, and A. Elzanaty, "MU-Massive MIMO With Multiple RISs: SINR Maximization and Asymptotic Analysis," IEEE Wirel. Commun. Lett., vol. 12, no. 6, pp. 997–1001, 2023, doi: 10.1109/LWC.2023.3256187.

[28] A. Papazafeiropoulos, P. Kourtessis, and S. Chatzinotas, "Max-Min SINR Analysis of STAR-RIS Assisted Massive MIMO Systems with Hardware Impairments," IEEE Trans. Wirel. Commun., pp. 1–13, 2023, doi: 10.1109/TWC.2023.3316707.

[29] S. Fang, G. Chen, P. Xu, J. Tang, and J. A. Chambers, "SINR Maximization for RIS-Assisted Secure Dual-Function Radar Communication Systems," 2021 IEEE Glob. Commun. Conf. GLOBECOM 2021 - Proc., no. September, 2021, doi: 10.1109/GLOBECOM46510.2021.9685487.

[30] A. Subhash, A. Kammoun, A. Elzanaty, S. Kalyani, Y. H. Al-Badarneh, and M. S. Alouini, "Max-Min SINR Optimization for RIS-Aided Uplink Communications with Green Constraints," IEEE Wirel. Commun. Lett., vol. 12, no. 6, pp. 942–946, 2023, doi: 10.1109/LWC.2023.3244519.

[31] B. Guo, R. Li, and M. Tao, "Joint design of hybrid beamforming and phase shifts in ris-aided mmWave communication systems," IEEE Wirel. Commun. Netw. Conf. WCNC, vol. 2021-March, pp. 1–13, 2021, doi: 10.1109/WCNC49053.2021.9417417.

[32] Q. U. A. Nadeem, A. Kammoun, A. Chaaban, M. Debbah, and M. S. Alouini, "Asymptotic max-min SINR analysis of reconfigurable intelligent surface assisted MISO systems," IEEE Trans. Wirel. Commun., vol. 19, no. 12, pp. 7748–7764, 2020, doi: 10.1109/TWC.2020.2986438.

[33] M. A. Suliman, and S. A. Ayoob, "A comparison study between the downlink packet scheduling algorithms in LTE networks," Al-Rafidain Engineering Journal (AREJ), vol. 23, no. 3, pp. 27-40, 2015. doi:10.33899/rengj.2015.101568.

[34] Y. Pan, C. Pan, S. Jin, and J. Wang, "RIS-Aided Near-Field Localization and Channel Estimation for the Terahertz System," IEEE J. Sel. Top. Signal Process., vol. 17, no. 4, pp. 878–892, 2023, doi: 10.1109/JSTSP.2023.3285431.

[35] I. Yildirim, A. Uyrus, and E. Basar, "Modeling and Analysis of Reconfigurable Intelligent Surfaces for Indoor and Outdoor Applications in Future Wireless Networks," IEEE Trans. Commun., vol. 69, no. 2, pp. 1290–1301, 2021, doi: 10.1109/TCOMM.2020.3035391.

[36] S. Zeng, H. Zhang, B. Di, Z. Han, and L. Song, "Reconfigurable Intelligent Surface (RIS) Assisted Wireless Coverage Extension: RIS Orientation and Location Optimization," IEEE Commun. Lett., vol. 25, no. 1, pp. 269–273, 2021, doi: 10.1109/LCOMM.2020.3025345.

[37] K. Ntontin, A. A. A. Boulogeorgos, D. G. Selimis, F. I. Lazarakis, A. Alexiou, and S. Chatzinotas, "Reconfigurable Intelligent Surface Optimal Placement in Millimeter-Wave Networks," IEEE Open J. Commun. Soc., vol. 2, pp. 704–718, 2021, doi: 10.1109/OJCOMS.2021.3068790.

[38] K. Ntontin, A. A. A. Boulogeorgos, D. G. Selimis, F. I. Lazarakis, A. Alexiou, and S. Chatzinotas, "Reconfigurable Intelligent Surface Optimal Placement in Millimeter-Wave Networks," IEEE Open J. Commun. Soc., vol. 2, no. March, pp. 704–718, 2021, doi: 10.1109/OJCOMS.2021.3068790.

[39] G. C. Trichopoulos et al., "Design and Evaluation of Reconfigurable Intelligent Surfaces in Real-World Environment," IEEE Open J. Commun. Soc., vol. 3, no. February, pp. 462–474, 2022, doi: 10.1109/OJCOMS.2022.3158310.

[40] R. A. Abed and S. A. Ayoob, "Millimeter Wave Beams Coordination and Antenna Array Height Effect," AIP Conf. Proc., vol. 2830, no. 1, 2023, doi: 10.1063/5.0157290.

[41] R. A. Abed and S. A. Ayoob, "A Proposed Method to Coordinate mmWave Beams Based on Coordinated Multi-Point in 5G Networks," J.

Commun., vol. 17, no. 11, pp. 925–932, 2022, doi: 10.12720/jcm.17.11.925-932.

[42] C. A. Balanis, "Antenna Theory Analysis and Design," A John Wiley & Sons, Inc., Publication, Third Edition, New Jersey, 2005.

[43] Q. Xue, B. Li, X. Zuo, Z. Yan, and M. Yang, "Cell capacity for 5G cellular network with inter-beam interference," ICSPCC 2016 - IEEE Int. Conf. Signal Process. Commun. Comput. Conf. Proc., pp. 1–5, 2016, doi: 10.1109/ICSPCC.2016.7753608.

[44] X. Zuo, B. Li, Z. Yan, Q. Xue, and M. Yang, "Beam coordinated multi-points transmission for 5G millimeter-wave network," 2017 IEEE Int. Conf. Signal Process. Commun. Comput. ICSPCC 2017, vol. 2017-Janua, pp. 1–4, 2017, doi: 10.1109/ICSPCC.2017.8242483.

Bushra J. Qeryaqos was born in 1998 in Ninevah, Iraq. She earned her B.Sc. in Communication Engineering in 2020 from the Electrical Engineering Department at the University of Mosul. Currently, she is pursuing an M.Sc. in the same department. Her research interests focus on millimeter-wave technology and reconfigurable intelligent surfaces (RIS).

Saad A. Ayoob was born in Ninevah Province, Iraq, in 1972. He received his B.S. degree from the University of Mosul, Iraq, in 1996 and his M.S. degree and Ph.D. from the same University in 2005 and 2011 respectively, both in Communication engineering. He is currently an Assistant Prof. in the Electrical Engineering Department, University of Mosul. His research interests include Networking, millimeter-wave, 5G, 6G, Microstrip Patch Antenna, Reflective Intelligent Surfaces (RIS) and Communication systems.